JACS
JOURNAL OF THE AMERICAN CHEMICAL SOCIETY
Article
pubs.acs.org/JACS

One-pot Synthesis of Metal–Organic Frameworks with Encapsulated Target Molecules and Their Applications for Controlled Drug Delivery

Haoquan Zheng,[*,†,§] Yuning Zhang,[‡,§] Leifeng Liu,[†] Wei Wan,[†] Peng Guo,[†] Andreas M. Nyström,[*,‡] and Xiaodong Zou[*,†]

[†]Berzelii Center EXSELENT on Porous Materials, Department of Materials and Environmental Chemistry, Stockholm University, SE−106 91 Stockholm, Sweden

[‡]Institute of Environmental Medicine, Karolinska Institutet, SE-171 77 Stockholm, Sweden

Supporting Information

ABSTRACT: Many medical and chemical applications require target molecules to be delivered in a controlled manner at precise locations. Metal–organic frameworks (MOFs) have high porosity, large surface area, and tunable functionality and are promising carriers for such purposes. Current approaches for incorporating target molecules are based on multistep postfunctionalization. Here, we report a novel approach that combines MOF synthesis and molecule encapsulation in a one-pot process. We demonstrate that large drug and dye molecules can be encapsulated in zeolitic imidazolate framework (ZIF) crystals. The molecules are homogeneously distributed within the crystals, and their loadings can be tuned. We show that ZIF-8 crystals loaded with the anticancer drug doxorubicin (DOX) are efficient drug delivery vehicles in cancer therapy using pH-responsive release. Their efficacy on breast cancer cell lines is higher than that of free DOX. Our one-pot process opens new possibilities to construct multifunctional delivery systems for a wide range of applications.

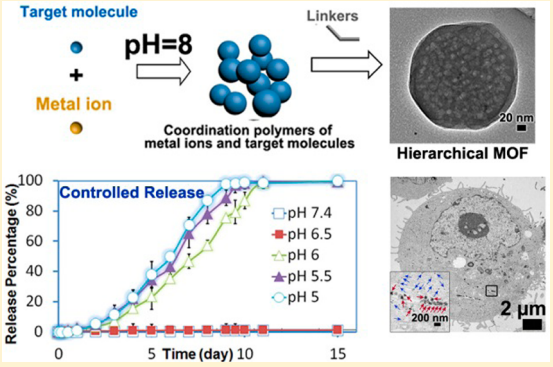

INTRODUCTION

Metal–organic frameworks (MOFs) have great potential in many applications, such as gas separation and storage,[1−4] catalysis,[5,6] sensing,[7] and drug delivery.[8−10] Their advantageous properties include structural diversity, large surface area, and tunable pore sizes and functionalities.[11−15] MOFs have been used as carriers of metal nanoparticles for catalysis[16,17] and of organic molecules such as drugs[9] and proteins[18] for medical applications. The encapsulation of target molecules by MOFs is currently achieved using a process that includes several steps: (1) synthesis of MOFs, (2) removal of solvents from the pores, and (3) incorporation of target molecules, which are often dissolved in toxic organic solvents. This process is both costly and produces large amounts of waste. Another drawback is the small pore window of MOFs, which limits their potential to encapsulate large molecules. In addition, the current loading capacity of large molecules in MOFs is lower than that of other inorganic carriers, such as mesoporous silica. A strategy to overcome these drawbacks is to combine MOF synthesis and molecule encapsulation into a one-pot process.[18−22]

Zeolitic imidazolate frameworks (ZIFs) are a subclass of MOFs, with high thermal and hydrothermal stabilities.[23−26] ZIFs have been used in gas separation[27] and as carriers for metal nanoparticles[28] and drugs.[29] ZIF-8 is a nontoxic and biocompatible ZIF built from zinc ions and 2-methylimidazolate and is a potential carrier for anticancer drugs.[30,31] ZIF-8 is stable under physiological conditions and decomposes under acidic conditions, which can be used to construct pH-sensitive drug delivery systems.[29] However, the diameter of the pore opening of ZIF-8 is 3.4 Å, and the diameter of the pore cavity is 11.6 Å, and thus large molecules cannot enter the pores. Several postsynthetic approaches have been developed to overcome this limitation, such as preparing hollow ZIFs and adsorbing molecules onto the external surfaces. However, postsynthesis approaches result in low loadings and rapid or poorly controlled release of the molecules.[29,31,32] Hierarchical structures can be introduced into MOFs,[33−36] which may lead to increased molecular loading. Further, hierarchical mesoporous silica can improve the molecular loading and the efficacy of drug delivery.[37] However, a certain rate of release of drugs still occurs at high pH (pH = 8). It is desirable to construct a pH-responsive drug delivery system that does not release drugs under physiological conditions in the circulation but that releases the drugs in a controlled manner after uptake of the system into selected cells, such as cancer cells. Such a system would reduce the systemic side effects of chemotherapy, as the active components are released only in the tumor region

Received: November 9, 2015
Published: December 28, 2015

DOI: 10.1021/jacs.5b11720
J. Am. Chem. Soc. 2016, 138, 962−968

and not in the general circulation.[38] However, no simple procedure to construct such a system has been developed.

We report here a simple and rapid process that combines the synthesis of ZIFs and the encapsulation of target organic molecules in one pot. The process has been used for two ZIFs, ZIF-8 and ZIF-67, and with four types of molecules with different functional groups. Electron tomography shows that homogeneously distributed mesopores can be generated within ZIF-8 crystals, and the size of the mesopores can be controlled by the loading of the molecules. We demonstrate that ZIF-8 crystal with encapsulated DOX (denoted DOX@ZIF-8) is a promising pH-responsive drug delivery system for cancer therapy. DOX@ZIF-8 does not release the drug under physiological conditions (pH ≈ 7.4) and releases it during a period of 7−9 days at pH 5.0−6.0. This is within the pH range of the endosome and lysosome. The release is achieved by successive decomposition of ZIF-8. The efficacy of the DOX@ZIF-8 system was further demonstrated by in vitro cell assays in three breast cancer cell lines and in primary macrophages. The cellular uptake of DOX@ZIF-8 was demonstrated by confocal microscopy and flow cytometry.

EXPERIMENTAL SECTION

Synthesis of DOX@ZIF-8. Stock solutions of DOX of different concentrations (2, 6, and 10 mg mL^{-1}) were prepared in deionized H_2O. First, 0.2 g (0.66 mmol) of $Zn(NO_3)_2{\cdot}6H_2O$ was dissolved in 0.8 g of H_2O (pH 8, adjusted by NaOH). Then, 4 mL of DOX stock solution was added to the $Zn(NO_3)_2$ solution. After this had been stirred for 1 min, 10 g of a solution containing 2 g (24.36 mmol) of 2-methylimidazole (2-mim) and 8 g of deionized H_2O was added dropwise. The reaction mixture was stirred for 15 min. The precipitate was collected by centrifugal separation and washed at least three times with a mixture of ethanol and H_2O. The powder product was dried at room temperature under vacuum. The loading amount of DOX was tuned by changing the concentration of the DOX stock solution. DOX-free ZIF-8 was synthesized in a similar way for comparison, using 4 mL of deionized H_2O.

Synthesis of Dye@ZIF-8, DOX@ZIF-67 and ZIF-8 encapsulated with several components is described in detailed in the Supporting Information.

Release of DOX from DOX@ZIF-8 Particles at Different pHs. A typical release system was prepared by suspending 10 mg of DOX@ZIF-8 material in 20.0 mL of buffer solution (pH 7.4, 6.5, 6.0, 5.0 and 4.0, respectively) at 37 °C. The release system was then maintained at 37 °C under shaking (shaking frequency = 150 rpm). One mL of release medium was sampled at each time point, and UV−vis spectrophotometry was used to determine the percentage of DOX that had been released, after which the sample was returned to the original release system. In a stepped release experiment, 10 mg of DOX@ZIF-8 material was tested in a 20.0 mL, pH 7.4 buffer solution of 10% (v/v) FBS at 37 °C for 7 days. The pH of the solution was then adjusted to 6.5 with dilute HCl (0.6 M) and kept for another 7 days. The pH of the solution was again adjusted, stepwise over 3 days, to 6.0, 5.0, and 4.0. The amount of DOX loaded was determined from the UV−vis absorbance at 479 nm. The release percentages of DOX were calculated according to the formula, release percentage (%) = m_r/m_l, where m_r is the amount of released DOX, while m_l is the total amount of loaded DOX.

MTT Assays in Breast Cancer Cell Lines and Primary Macrophages. Monocytes were seeded onto 96-well plates with 1 × 10^5 cells per well, 3 days prior to the test, in order to derive macrophages. MCF-7, MDA-MB-231, and MDA-MB-468 cell lines were harvested with trypsin, washed with PBS, and resuspended in Dulbecco's modified eagle medium at a concentration of 1 × 10^5 cells per ml. 100 μL per well of the cell suspension was transferred into 96-well plates to preculture for 24 h. The medium was replaced by a fresh medium that contained the sample (DOX, DOX@ZIF-8, ZIF-8, or ZIF-8 + DOX) at various concentrations. 10 μL of 5 mg mL^{-1} MTT (3-(4,5,-dimethylthiazol-2-yl)-2,5-diphenyltetrazolium bromide) was then added to each well after designated incubation periods (12 and 24 h for the macrophages, and 24 and 72 h for the cell lines). After 4 h, 100 μL of 10% sodium dodecyl sulfate solution was introduced into each well. The absorbance at 570 nm was determined with a plate reader after 18 h.

Confocal Microscopy. MDA-MB-468 cells were seeded at a concentration of 1 × 10^6 cells per well onto the surface of coverslips placed in 12-well plates and precultured for 24 h at 37 °C. The medium was removed, and fresh medium that contained free DOX (0.2 μg mL^{-1}) or DOX@ZIF-8 (1 μg mL^{-1}, 20 wt % loading) was added. After 2, 8, or 24 h of incubation, the cells were washed twice with PBS and fixed with 4% paraformaldehyde in PBS for 15 min at room temperature. The cells were then stained with 2.5 μg mL^{-1} of 4′,6-diamidino 2-phenylindole (DAPI) for 10 min and mounted with ProLong Gold antifade mounting medium. The stained samples were examined in an FV1000 Olympus confocal microscope at excitation/emission wavelengths of 405/461 nm for DAPI and 559/572 nm for DOX. Images were acquired and analyzed with the FluoView FV1000 software.

RESULTS AND DISCUSSION

One-Pot Synthesis of Target Molecule Encapsulated in ZIF Crystals. The process for one-pot synthesis of MOFs with encapsulated target molecules is presented in Figure 1.

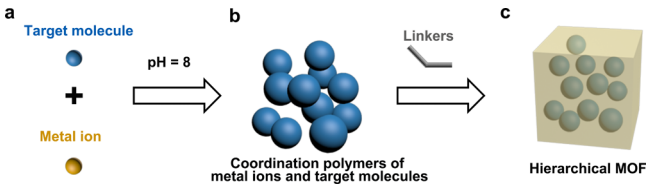

Figure 1. The pH-induced one-pot synthesis of MOFs with encapsulated target molecules.

Metal ions and target organic molecules (Figure 1a) self-assemble to form coordination polymers (Figure 1b). Organic linkers are added to disassemble the metal ions from the target organic molecules and subsequently form MOFs (Figure 1c) by the assembly of the metal ions and linkers. The target molecules are encapsulated during the formation of MOFs, resulting in hierarchical MOFs. Several molecules with different functional groups (a typical anticancer drug DOX, dye molecules rhodamine B, methyl orange, and methylene blue) (Figure S1) have been successfully encapsulated into ZIF-8 crystals.

We chose initially to study ZIF-8 as the carrier and DOX, a typical anticancer drug used in the treatment of breast and ovarian cancers,[39,40] as the target molecule. DOX molecules have functional groups that form weak coordination bonds with Zn^{2+} ions in aqueous media.[41,42] DOX@ZIF-8 particles were synthesized in pure aqueous solutions (Figure 2). In a typical synthesis, a solution of $Zn(NO_3)_2{\cdot}6H_2O$ (0.66 mmol, pH = 8 adjusted by NaOH) and a solution of DOX (0−30 wt %) was mixed and stirred for 1 min. A solution of 2-methylimidazole (2-mim, 24.36 mmol) was added dropwise. The reaction mixture was stirred for 15 min, and DOX@ZIF-8 particles were collected by centrifugal separation (see Table S1, the Experimental section and Supporting Information for detailed descriptions). DOX@ZIF-8 particles with loadings of up to 20% were achieved (Figure 2). We confirmed that DOX molecules were coordinated with Zn^{2+} ions by examining the red shift of the UV−vis spectrum and comparing it with that of

DOI: 10.1021/jacs.5b11720
J. Am. Chem. Soc. 2016, 138, 962−968

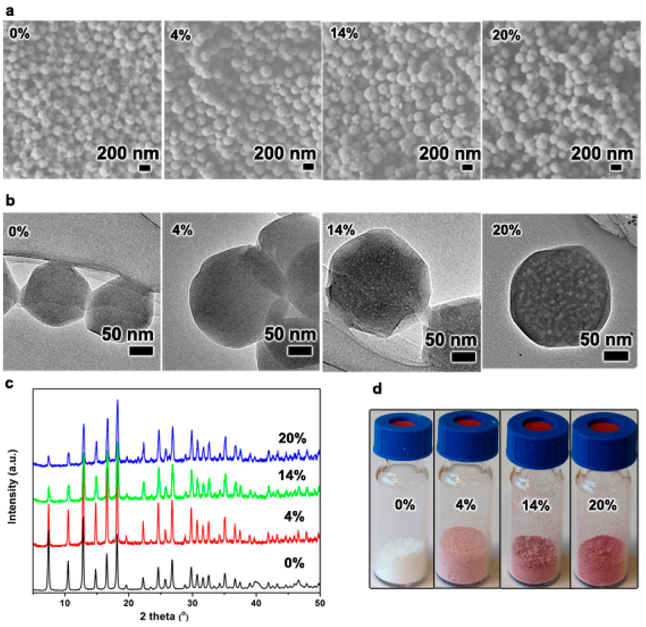

Figure 2. (a) SEM and (b) TEM images, (c) PXRD patterns, and (d) photographs of DOX@ZIF-8 particles with 0, 4, 14, and 20% DOX loadings.

a free DOX solution, while the solid-state UV−vis spectrum of DOX@ZIF-8 showed that there was no coordination bond between DOX and Zn^{2+} ions in DOX@ZIF-8 (Figure S2). Our micro/mesostructured DOX@ZIF-8 has one of the highest DOX loadings among MOF carriers.

Scanning electron microscopy (SEM) showed that the DOX@ZIF-8 materials consisted of isolated crack-free particles of diameter 70−300 nm (Figure 2a). Powder X-ray diffraction (PXRD) showed that the DOX@ZIF-8 particles were of high crystallinity with sharp diffraction peaks (Figure 2c). The decrease of the peak intensity at the low angles for ZIF-8 with 14 and 20% DOX loadings was due to the presence of DOX molecules in the pores of ZIF-8 crystals. No diffraction peaks from the DOX molecules were observed, indicating that no DOX crystals were present in the DOX@ZIF-8 materials. The color of the DOX@ZIF-8 particles became more intense with higher DOX concentration (Figure 2d). This indicates that the target molecules have been successfully loaded into the ZIF crystals. While the morphology of ZIF-8 crystals did not change with increasing loading of DOX (from 0% to 20%), the particle size increased and the size distribution broadened (from 100 ± 30 to 230 ± 150 nm), as shown by dynamic light scattering (DLS, Figure S3a). All these particles were highly dispersed and stable in water and PBS (pH 7.4), as a result of their high ζ potentials (+30.5, +30.1, +30.7, and +31.1 mV for 0, 4, 14 and 20% loadings, respectively). Because salts in the blood may cause agglomeration of nanoparticles,[43] the particle sizes were measured by DLS in the presence of 0.9% NaCl (Figure S3b). We found that the particle sizes only increased slightly, by no more than three times on average. The good dispersion of the particles in cells was also confirmed by TEM (Figure 6b).

Transmission electron microscopy (TEM) showed well-defined mesopores that were homogeneously distributed within the ZIF-8 crystals when the loadings were high (≥14%, Figure 2b). The size of the mesopores increased with the loading of DOX. Notably, despite the presence of large amounts of mesopores, each ZIF-8 particle was a single crystal, which was confirmed by electron diffraction (Figure S4). Electron tomography showed that each ZIF-8 crystal consisted of a core with isolated and homogeneously distributed mesopores and a mesopore-free shell (Figure 3, Figure S5, and Videos S1, S2, S3, and S4). For DOX@ZIF-8 with 20% loadings, the diameter of the mesopores, in which the DOX molecules were located, was 5−15 nm. The mesopore-free shell was approximately 20 nm thick, which is the result of depletion of target molecules and was not observed when a shorter synthesis time was used (Figure S6).

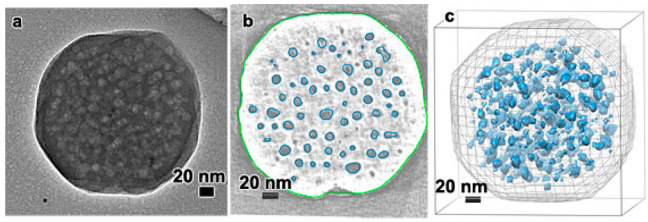

Figure 3. Distribution of mesopores in DOX@ZIF-8 particles illustrated by electron tomography. (a) TEM image of a DOX@ZIF-8 single crystal. (b) Cross-section of the electron tomogram with the mesopores marked by blue lines. (c) 3D distribution of the mesopores in the DOX@ZIF-8 particles.

We demonstrated the versatility of our one-pot encapsulation process by using it with other organic molecules. Three dye molecules, rhodamine B, methyl orange, and methylene blue, were chosen, all of which have functional groups that can form weak coordination bonds with Zn^{2+} ions in aqueous media (Figure S7). In all cases, micro/mesostructured ZIF-8 crystals with encapsulated dye were successfully synthesized, with loadings of 15, 14 and 17% for rhodamine B, methyl orange, and methylene blue, respectively (Table S1 and Figure S8). We also tested whether our process can be applied to other metal ions and used cobalt ions instead of zinc ions, with the same organic linker 2-mim, to synthesize DOX@ZIF-67. Hierarchical micro/mesostructured DOX@ZIF-67 material with a DOX loading of 15% was synthesized in an aqueous solution (Figure S9). We conclude that our one-pot process can be generally used to synthesize micro/mesostructured ZIF materials with encapsulated target organic molecules.

Our simple one-pot synthesis allows the simultaneous incorporation of several molecules and nanoparticles into the same MOF crystals. It is possible to encapsulate metal nanoparticles and DOX in ZIF-8 crystals in one pot (Figure S10). Furthermore, the encapsulated organic molecules can be removed, leading to hierarchical micro/mesoporous ZIF-8 materials (Figure S11), which can improve the diffusion and mass transfer properties.

The pH-Responsive Release of DOX from DOX@ZIF-8 Particles. We studied the potential of DOX@ZIF-8 as a drug delivery system for cancer therapy, because ZIF-8 is stable under physiological conditions (pH ≈ 7.4) and decomposes under acidic conditions. Figure 4a shows the pH-responsive cumulative release profiles of DOX@ZIF-8 with 20% DOX loading. There is virtually no release of DOX (<1%) from DOX@ZIF-8 even after 15 days at a pH equal or higher than 6.5 in phosphate-buffered saline (PBS) with 10% (v/v) fetal bovine serum (FBS) at 37 °C. At low pH (5.0−6.0), DOX was released at a steady rate, with more than 95% of the DOX being released during 7−9 days. There was an induction period of about 2 days, during which the DOX release was very low

DOI: 10.1021/jacs.5b11720
J. Am. Chem. Soc. 2016, 138, 962−968

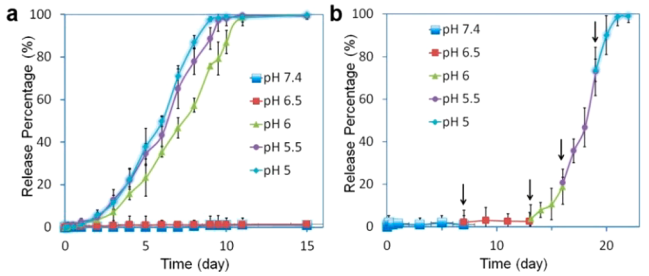

Figure 4. The pH-responsive release of DOX from DOX@ZIF-8 particles determined by UV−vis spectrophotometry. (a) The typical release system. (b) The stepped release system. Results are presented as means ± standard deviation (SD) (n = 3).

(<2%). The release mechanism of the present DOX@ZIF-8 system is different from that in other drug delivery systems, such as mesoporous silica[44] and other MOFs.[8] The release of drugs from DOX@ZIF-8 at low pH is associated with the dissolution of ZIF-8. The induction period is associated with the dissolution of the peripheral DOX-free shells of ZIF-8, which act as a protective capsule around the DOX@ZIF-8. In the cases of mesoporous silica and other MOFs, drugs are released through the pores, and the drug carriers remain intact. One important advantage of our DOX@ZIF-8 system is that the DOX molecules are safely stored with essentially no release under physiological conditions. DOX@ZIF-8 is stable, and no DOX is released even at 60 °C during 7 days in PBS at pH 7.4 (Figure S12). Another advantage is that high loading can be achieved using the one-pot process presented here. The highest DOX loading (29%) reported in a drug delivery system has been achieved with MIL-100 (Fe), where DOX is located in the intrinsic mesopores of the MOF framework. However, more than 95% of DOX was released under physiological conditions during 5 days.[8] The unique release property of DOX@ZIF-8 makes it interesting as a potential pH-responsive drug delivery system for cancer therapy. The DOX molecules may be retained in the ZIF-8 crystals as they circulate in the bloodstream (where the pH ≈ 7.4 in physiological conditions) and be slowly released after the accumulation of DOX@ZIF-8 in tumor cells, where the pH values in intracellular organelles are lower (pH = 5−6).[45] The process of transfer from the circulation in the bloodstream to the endosome and lysosome compartments was mimicked by a gradual acidification of release media from pH 7.4 to 5.0, by the addition of dilute HCl (Figure 4b). The cumulated release of DOX remained very low (<1%) as the pH was lowered from 7.4 to 6.5. It increased sharply when the pH value was lowered to 6.0, 5.5, and finally 5.0. This confirms that DOX@ZIF-8 is a promising pH-responsive drug delivery system. It is worth mentioning that free DOX dissolved completely in <1 h at 37 °C in PBS at the pH range of 5.0−7.4 (Figure S13). We conclude that the slow release of DOX from DOX@ZIF-8 is indeed due to the release of the DOX molecules encapsulated in ZIF-8. No zinc ions were present in PBS pH 7.4 after 11 days of storage (Figure S14), which indicates that DOX@ZIF-8 is very stable. Zinc ions are, however, released in the acidic medium (pH = 5.0), as a result of the dissolution of the DOX@ZIF-8 particles, and 98% of the zinc ions have been released after 11 days (Figure S14). This confirms that the drug release is indeed triggered by pH, through breakage of the coordination bonds between zinc and imidazolate. Our results agree with previous stability studies of the pH-responsive ZIF-8.[32]

Cytotoxicity Tests. The cytotoxicities of DOX@ZIF-8, free DOX, pure ZIF-8, and a mixture of free DOX and ZIF-8 were evaluated by determining cellular viability using an MTT assay, which measures the mitochondrial function of the cells. We first tested the cytotoxic effect of ZIF-8 crystals that had been degraded for 24 or 72 h in PBS at pH = 5 and 37 °C, following incubation periods of 3 or 11 days (Figure S15). The cellular viability decreased with the concentration of ZIF-8, degradation time, and incubation time. At relatively high concentrations (up to 250 μg mL^{-1} fully dissolved ZIF-8), the viability was still high, 75−90%. It decreased rapidly at higher concentrations (≥500 μg mL^{-1}) and prolonged incubation time. We compared the toxicities of DOX@ZIF-8, a mixture of ZIF-8 and free DOX (denoted ZIF-8+DOX), pure ZIF-8, and free DOX on primary macrophages and three breast cancer cell lines (MDA-MB-231, MDA-MB-468, and MCF-7), treated for 24 or 72 h (Figures 5

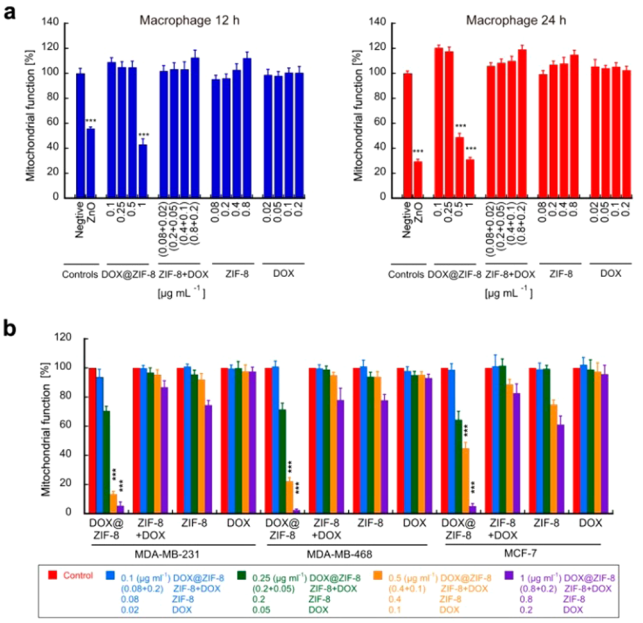

Figure 5. Comparison of the mitochondrial function in macrophages and breast cancer cells exposed to DOX@ZIF-8, a mixture of ZIF-8 and DOX (ZIF-8 + DOX), pure ZIF-8, or free DOX. (a) The function of mitochondria in macrophages treated for 12 or 24 h. (b) The function of mitochondria in the breast cancer cell lines MCF-7, MDA-MB-231, and MDA-MB-468 treated for 24 h.

and S16). We found that DOX@ZIF-8 was toxic in a dose-dependent manner to the macrophages (Figure 5a) and to the three breast cancer cell lines (Figure 5b). After treatment with DOX@ZIF-8 at a concentration of 0.5 μg mL^{-1} (equivalent to a concentration of DOX of 0.1 μg mL^{-1}) for 24 h, the mitochondrial function fell from the baseline level to 16% in MDA-MB-231, to 20% in MDA-MB-468, and to 43% in MCF-7 cells (Figure 5b). The values were even lower (below 10%) after the cells had been treated with DOX@ZIF-8 at a concentration of 1 μg mL^{-1} (Figure 5b). Further, the mitochondrial in the three breast cancer cell lines almost ceased to function after treatment with DOX@ZIF-8 at a concentration of 0.5 or 1 μg mL^{-1} for 72 h (Figure S16). Mitochondrial function in cells treated with equivalent concentrations of free DOX, ranging from 0.02 to 0.2 μg mL^{-1}, was not affected after 24 h (Figure 5b). However, after 72 h incubation time, DOX induced a dose-dependent loss of

DOI: 10.1021/jacs.5b11720
J. Am. Chem. Soc. 2016, 138, 962−968

mitochondrial function (Figure S16). After treatment with ZIF-8 at a concentration of 0.8 μg mL^{-1}, the mitochondrial function fell to 76% from the baseline level in MDA-MB-231, to 68% in MDA-MB-468, and to 60% in MCF-7 cells (Figure S16). The toxic effect of DOX@ZIF-8 was significantly higher after 24 h than the toxic effects of ZIF-8 and free DOX. The greater efficacy was not caused by the simple additive effect of ZIF-8 and DOX, as shown by experiments using the same assay for the mixture of free DOX and ZIF-8 at the same concentrations of ZIF-8 and DOX as in the drug-loaded DOX@ZIF-8 (Figure 5b). Mitochondrial function was only slightly affected at the DOX concentration range that was tested (from 0.02 to 0.2 μg mL^{-1}) after 24 h exposure. The mixture of ZIF-8 and DOX did have a dose-dependent effect, but we believe that this was induced by free DOX, since the trend for the mixture of ZIF-8 and DOX was similar to that of free DOX (Figure S16). We conclude that DOX@ZIF-8 has a cytotoxicity for the three breast cancer cell lines that is 14−37 fold ($p < 0.001$) greater than other systems. This increase is not a result of the effects of pure ZIF-8 or the mixture of ZIF-8 and DOX, but a result of a synergistic effect of DOX and ZIF-8 in DOX@ZIF-8.

We studied the apoptosis/necrosis of the cells treated with DOX@ZIF-8, ZIF-8 + DOX, ZIF-8, or free DOX in order to confirm our conclusion. These experiments were carried out using fluorescence-activated cell sorting (Figures S17−20, with a summary in Figure S21). DOX@ZIF-8 at a concentration of 0.5 μg mL^{-1} induced significant ($p < 0.001$) necrosis in the human macrophages after 24 h and significant ($p < 0.001$) apoptosis in the breast cancer cell lines after 24 h (MDA-MB-231 and MDA-MB-468) or 48 h (MCF-7). The apoptosis induced by DOX@ZIF-8 in the breast cancer cells was significantly higher than the necrosis, which indicates DOX@ZIF-8 can trigger programmed cell death (apoptosis) rather than random, rapid cell death (necrosis). And the enhanced apoptosis of cancer cells is usually considered as a sign of the drug efficacy. The drug-loaded carriers are suitable for cancer therapy, after appropriate modification to lower the uptake and consequent toxic effects of DOX@ZIF-8 in macrophages.[46] One possible strategy is to attach a pharmacokinetic modifier, poly(ethylene glycol) (PEG), onto the surfaces of the DOX@ZIF-8 particles. Such a modification may enhance the biocompatibility of the particles and prolong their blood circulation time, through a reduction in protein adsorption or avoiding uptake by the reticuloendothelial system.[46,47] This may promote the accumulation of the particles in tumors since the permeability is higher and the retention (EPR) longer.[48]

Cellular Uptake of DOX@ZIF-8. We compared the uptake of free DOX and DOX@ZIF-8 into the cells by confocal microscopy. The MDA-MB-468 cell line was selected because its sensitivity to DOX@ZIF-8 is higher and its sensitivity to ZIF-8 is lower than the other two cell lines. Free DOX entered the nuclei very fast (within 2 h) and accumulated in the nuclei, as shown by the significant colocalization of DOX and DAPI (Figure 6a). The intensity of the signal generated by DOX increased with the incubation time (from 2 to 24 h), and DOX was always located in the nuclei. Moreover, the nuclei did not fragment to a significant extent during this period, indicating that DOX does not induce apoptosis in MDA-MB-468 cells within 24 h. This is consistent with the MTT results after 24 h of treatment with free DOX (Figure 5a). The uptake of DOX@ZIF-8 differed from that of free DOX. DOX@ZIF-8 particles were present only in the cytoplasm after 2 h and accumulated around the cell nuclei after 4 h (Figure 6a). DOX@ZIF-8

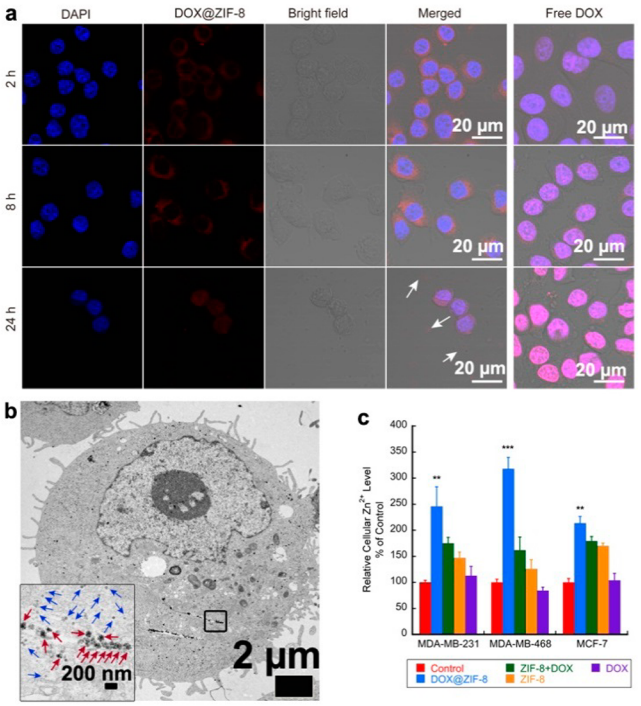

Figure 6. Uptake studies of DOX@ZIF-8 in breast cancer cells. (a) Comparison of the localizations of DOX@ZIF-8 and free DOX in the MDA-MB-468 cells. (b) TEM image of an MDA-MB-468 cell. The inset is an enlarged image of the area marked by the square showing individual ZIF-8 particles (blue arrows) and their aggregates (red arrows). (c) Relative Zn^{2+} levels in the breast cancer cells after different treatments for 24 h. Results are presented as means ± SD (n = 4).

particles cannot initially enter the nuclei. Most cells were dead after 24 h of treatment, and only cellular debris was present. The few cells that were present had irregularly shaped nuclei and a small volume of cytoplasm. DOX@ZIF-8 was distributed equally between the nuclei and cytoplasm at this stage and in the cell debris (indicated by arrows in Figure 6a, 24 h). This rapid and total cellular disruption by DOX@ZIF-8 confirms the MTT results shown in Figure 5b, in which the function of the mitochondria is 5% of baseline for a concentration of DOX@ZIF-8 of 1 μg mL^{-1} in MDA-MB-468 cells. The difference in distribution patterns of DOX in the cells treated with free DOX and DOX@ZIF-8 shows that ZIF-8 alters the DOX delivery pathway in the cells. This may explain why DOX@ZIF-8 has a stronger effect and induces cell death more rapidly than the other agents. TEM images confirmed the intracellular uptake of the ZIF-8 particles into the MDA-MB-468 cells (Figure 6b). We selected a concentration of DOX@ZIF-8 of 8 μg mL^{-1} and an incubation time of 2 h because the cells were still intact under these conditions and suitable for the observation of cellular uptake. The ZIF-8 particles were localized mainly in the cytoplasm and subcellular organelles and were smaller than the as-prepared ZIF-8 particles, presumably due to partial dissolution of ZIF-8 particles in the cells.

We quantified the uptake of ZIF-8 particles into the cells by measuring the relative cellular Zn^{2+} level (Figure 6c). FluoZin-3 fluorescence indicators were loaded into cells treated with DOX@ZIF-8 or ZIF-8, and the intensity of the fluorescence was measured, normalized for the protein mass of each well in the cell culture plate. The relative fluorescence intensities from cells treated with DOX@ZIF-8, ZIF-8, or ZIF-8+DOX were

DOI: 10.1021/jacs.5b11720
J. Am. Chem. Soc. 2016, 138, 962−968

significantly higher. Interestingly, the level of Zn^{2+} in cells treated with DOX@ZIF-8 was significantly higher than in cells treated with ZIF-8+DOX or ZIF-8 (Figure 6c).

CONCLUSION

We have developed a simple, one-pot process for the synthesis of ZIFs that contain encapsulated organic molecules. Four substances, the anticancer drug DOX and three organic dyes, have been successfully encapsulated in the ZIFs with high loadings (14−20 wt %). The resulting ZIF crystals have hierarchical pore structures, which consist of ordered micropores that are intrinsic to the ZIF framework, and homogeneously distributed mesopores filled by target molecules. The size of the mesopores can be tuned by changing the concentration of the target molecules. The target molecules can be extracted, leading in hierarchical micro/mesoporous ZIF-8 materials. We have shown that ZIF-8 crystals loaded with DOX can be used as an efficient pH-responsive drug delivery system, in which the drug is not released at physiological condition (PBS, pH 7.4) and released in a controlled manner at low pH (5.0−6.5). The DOX@ZIF-8 system shows a synergistic effect, and its cytotoxicity is higher than free DOX.

We have also demonstrated that metal nanoparticles and target molecules can be encapsulated simultaneously into ZIFs using the one-pot process. The process can be used for other functional species, such as magnetic particles, quantum dots, metal oxides, or enzymes. This opens new opportunities to develop multifunctional materials for applications in, for example, drug delivery, heterogeneous catalysis, the removal of organic contaminants, bioimaging, etc. The synthesis is simple, scalable, and environmentally friendly and has strong potential for industrial applications.

ASSOCIATED CONTENT

Supporting Information

The Supporting Information is available free of charge on the ACS Publications website at DOI: 10.1021/jacs.5b11720.

The synthetic procedures, more characterization results and cytotoxicity tests of DOX@ZIF-8 crystals (PDF)
(AVI)
(AVI)
(AVI)
(AVI)

AUTHOR INFORMATION

Corresponding Authors

*haoquan.zheng@mmk.su.se
*Andreas.nystrom470@gmail.com
*xzou@mmk.su.se

Author Contributions

§These authors contributed equally.

Notes

The authors declare no competing financial interest.

ACKNOWLEDGMENTS

The project is supported by the Swedish Research Council (VR), the Swedish Governmental Agency for Innovation Systems (VINNOVA), and the Knut & Alice Wallenberg Foundation through the project grant 3DEM-NATUR and a grant for purchasing the TEM. Funding support to A.M.N. by the Royal Swedish Academy of Sciences, and the Swedish Research Council (VR) under grant 2011-3720 is gratefully acknowledged. A.M.N. is the recipient of a senior research fellowship from Karolinska Institutet and the Institute of Environmental Medicine.

REFERENCES

(1) Rosi, N. L.; Eckert, J.; Eddaoudi, M.; Vodak, D. T.; Kim, J.; O'Keeffe, M.; Yaghi, O. M. *Science* **2003**, *300*, 1127.
(2) Murray, L. J.; Dinca, M.; Long, J. R. *Chem. Soc. Rev.* **2009**, *38*, 1294.
(3) Farha, O. K.; Yazaydın, A. Ö.; Eryazici, I.; Malliakas, C. D.; Hauser, B. G.; Kanatzidis, M. G.; Nguyen, S. T.; Snurr, R. Q.; Hupp, J. T. *Nat. Chem.* **2010**, *2*, 944.
(4) Yang, S.; Lin, X.; Lewis, W.; Suyetin, M.; Bichoutskaia, E.; Parker, J. E.; Tang, C. C.; Allan, D. R.; Rizkallah, P. J.; HUbberstey, P.; Champness, N. R.; Thomas, K. M.; Blake, A. J.; Schröder, M. *Nat. Mater.* **2012**, *11*, 710.
(5) Lee, J.; Farha, O. K.; Roberts, J.; Scheidt, K. A.; Nguyen, S. T.; Hupp, J. T. *Chem. Soc. Rev.* **2009**, *38*, 1450.
(6) Xiao, D. J.; Bloch, E. D.; Mason, J. A.; Queen, W. L.; Hudson, M. R.; Planas, N.; Borycz, J.; Dzubak, A. L.; Verma, P.; Lee, K.; Bonino, F.; Crocella, V.; Yano, J.; Bordiga, S.; Truhlar, D. G.; Gagliardi, L.; Brown, C. M.; Long, J. R. *Nat. Chem.* **2014**, *6*, 590.
(7) Allendorf, M. D.; Bauer, C. A.; Bhakta, R. K.; Houk, R. J. T. *Chem. Soc. Rev.* **2009**, *38*, 1330.
(8) Horcajada, P.; Chalati, T.; Serre, C.; Gillet, B.; Sebrie, C.; Baati, T.; Eubank, J. F.; Heurtaux, D.; Clayette, P.; Kreuz, C.; Chang, J.-S.; Hwang, Y. K.; Marsaud, V.; Bories, P.-N.; Cynober, L.; Gil, S.; Férey, G.; Couvreur, P.; Gref, R. *Nat. Mater.* **2010**, *9*, 172.
(9) Horcajada, P.; Gref, R.; Baati, T.; Allan, P. K.; Maurin, G.; Couvreur, P.; Férey, G.; Morris, R. E.; Serre, C. *Chem. Rev.* **2012**, *112*, 1232.
(10) McKinlay, A. C.; Morris, R. E.; Horcajada, P.; Férey, G.; Gref, R.; Couvreur, P.; Serre, C. *Angew. Chem., Int. Ed.* **2010**, *49*, 6260.
(11) Chen, B.; Xiang, S.; Qian, G. *Acc. Chem. Res.* **2010**, *43*, 1115.
(12) Farha, O. K.; Hupp, J. T. *Acc. Chem. Res.* **2010**, *43*, 1166.
(13) Férey, G.; Mellot-Draznieks, C.; Serre, C.; Millange, F.; Dutour, J.; Surblé, S.; Margiolaki, I. *Science* **2005**, *309*, 2040.
(14) Eddaoudi, M.; Moler, D. B.; Li, H.; Chen, B.; Reineke, T. M.; O'Keeffe, M.; Yaghi, O. M. *Acc. Chem. Res.* **2001**, *34*, 319.
(15) Chae, H. K.; Siberio-Perez, D. Y.; Kim, J.; Go, Y.; Eddaoudi, M.; Matzger, A. J.; O'Keeffe, M.; Yaghi, O. M. *Nature* **2004**, *427*, 523.
(16) Jiang, H.-L.; Liu, B.; Akita, T.; Haruta, M.; Sakurai, H.; Xu, Q. *J. Am. Chem. Soc.* **2009**, *131*, 11302.
(17) Dhakshinamoorthy, A.; Garcia, H. *Chem. Soc. Rev.* **2012**, *41*, 5262.
(18) Lyu, F.; Zhang, Y.; Zare, R. N.; Ge, J.; Liu, Z. *Nano Lett.* **2014**, *14*, 5761.
(19) Zhuang, J.; Kuo, C.-H.; Chou, L.-Y.; Liu, D.-Y.; Weerapana, E.; Tsung, C.-K. *ACS Nano* **2014**, *8*, 2812.
(20) Zheng, M.; Liu, S.; Guan, X.; Xie, Z. *ACS Appl. Mater. Interfaces* **2015**, *7*, 22181.
(21) Liédana, N.; Galve, A.; Rubio, C.; Téllez, C.; Coronas, J. *ACS Appl. Mater. Interfaces* **2012**, *4*, 5016.
(22) Ren, H.; Zhang, L.; Wang, T.; Li, L.; Su, Z.; Wang, C. *Chem. Commun.* **2013**, *49*, 6036.
(23) Huang, X.-C.; Lin, Y.-Y.; Zhang, J.-P.; Chen, X.-M. *Angew. Chem., Int. Ed.* **2006**, *45*, 1557.
(24) Lu, G.; Li, S.; Guo, Z.; Farha, O. K.; Hauser, B. G.; Qi, X.; Wang, Y.; Wang, X.; Han, S.; Liu, X.; DuChene, J. S.; Zhang, H.; ZHang, Q.; Chen, X.; Ma, J.; Loo, S. C. J.; Wei, W. D.; Yang, Y.; Hupp, J. T.; Huo, F. *Nat. Chem.* **2012**, *4*, 310.
(25) Park, K. S.; Ni, Z.; Côté, A. P.; Choi, J. Y.; Huang, R.; Uribe-Romo, F. J.; Chae, H. K.; O, O. X.; DuChene, J. S. *Proc. Natl. Acad. Sci. U. S. A.* **2006**, *103*, 10186.
(26) Zhang, J.-P.; Zhang, Y.-B.; Lin, J.-B.; Chen, X.-M. *Chem. Rev.* **2012**, *112*, 1001.
(27) Venna, S. R.; Carreon, M. A. *J. Am. Chem. Soc.* **2010**, *132*, 76.

DOI: 10.1021/jacs.5b11720
J. Am. Chem. Soc. 2016, 138, 962−968

(28) Chizallet, C.; Lazare, S.; Bazer-Bachi, D.; Bonnier, F.; Lecocq, V.; Soyer, E.; Quoineaud, A.-A.; Bats, N. *J. Am. Chem. Soc.* **2010**, *132*, 12365.
(29) Sun, C.-Y.; Qin, C.; Wang, X.-L.; Yang, G.-S.; Shao, K.-Z.; Lan, Y.-Q.; Su, Z.-M.; Huang, P.; Wang, C.-G.; Wang, E.-B. *Dalton Trans.* **2012**, *41*, 6906.
(30) Broadley, M. R.; White, P. J.; Hammond, J. P.; Zelko, I.; Lux, A. *New Phytol.* **2007**, *173*, 677.
(31) Ren, H.; Zhang, L.; An, J.; Wang, T.; Li, L.; Si, X.; He, L.; Wu, X.; Wang, C.; Su, Z. *Chem. Commun.* **2014**, *50*, 1000.
(32) Vasconcelos, I. B.; Silva, T. G. d.; Militao, G. C. G.; Soares, T. A.; Rodrigues, N. M.; Rodrigues, M. O.; Costa, N. B. d.; Freire, R. O.; Junior, S. A. *RSC Adv.* **2012**, *2*, 9437.
(33) Wu, Y.-n.; Zhou, M.; Zhang, B.; Wu, B.; Li, J.; Qiao, J.; Guan, X.; Li, F. *Nanoscale* **2014**, *6*, 1105.
(34) Wee, L. H.; Lescouet, T.; Ethiraj, J.; Bonino, F.; Vidruk, R.; Garrier, E.; Packet, D.; Bordiga, S.; Farrusseng, D.; Herskowitz, M.; Martens, J. A. *ChemCatChem* **2013**, *5*, 3562.
(35) Fang, Z.; Dürholt, J. P.; Kauer, M.; Zhang, W.; Lochenie, C.; Jee, B.; Albada, B.; Metzler-Nolte, N.; Pöppl, A.; Weber, B.; Muhler, M.; Wang, Y.; Schmid, R.; Fischer, R. A. *J. Am. Chem. Soc.* **2014**, *136*, 9627.
(36) Zhang, W.; Liu, Y.; Lu, G.; Wang, Y.; Li, S.; Cui, C.; Wu, J.; Xu, Z.; Tian, D.; Huang, W.; DuCheneu, J. S.; Wei, W. D.; Chen, H.; Yang, Y.; Huo, F. *Adv. Mater.* **2015**, *27*, 2923.
(37) Zhu, Y.; Shi, J.; Shen, W.; Dong, X.; Feng, J.; Ruan, M.; Li, Y. *Angew. Chem., Int. Ed.* **2005**, *44*, 5083.
(38) Helmlinger, G.; Yuan, F.; Dellian, M.; Jain, R. K. *Nat. Med.* **1997**, *3*, 177.
(39) Piccart-Gebhart, M. J.; Procter, M.; Leyland-Jones, B.; Goldhirsch, A.; Untch, M.; Smith, I.; Gianni, L.; Baselga, J.; Bell, R.; Jackisch, C.; Cameron, D.; Dowsett, M.; Barrios, C. H.; Steger, G.; Huang, C.-S.; Andersson, M.; Inbar, M.; Lichinitser, M.; Láng, I.; Nitz, U.; Iwata, H.; Thomssen, C.; Lohrisch, C.; Suter, T. M.; Rüschoff, J.; Sütő, T.; Greatorex, V.; Ward, C.; Straehle, C.; McFadden, E.; Dolci, M. S.; Gelber, R. D. *N. Engl. J. Med.* **2005**, *353*, 1659.
(40) Yap, T. A.; Carden, C. P.; Kaye, S. B. *Nat. Rev. Cancer* **2009**, *9*, 167.
(41) Xing, L.; Zheng, H.; Cao, Y.; Che, S. *Adv. Mater.* **2012**, *24*, 6433.
(42) Zheng, H.; Xing, L.; Cao, Y.; Che, S. *Coord. Chem. Rev.* **2013**, *257*, 1933.
(43) Caballero-Díaz, E.; Pfeiffer, C.; Kastl, L.; Rivera-Gil, P.; Simonet, B.; Valcárcel, M.; Jiménez-Lamana, J.; Laborda, F.; Parak, W. J. *Part. Part. Syst. Charact.* **2013**, *30*, 1079.
(44) Schlossbauer, A.; Warncke, S.; Gramlich, P. M. E.; Kecht, J.; Manetto, A.; Carell, T.; Bein, T. *Angew. Chem., Int. Ed.* **2010**, *49*, 4734.
(45) Yoshida, T.; Lai, T. C.; Kwon, G. S.; Sako, K. *Expert Opin. Drug Delivery* **2013**, *10*, 1497.
(46) Zhang, Y.; Kohler, N.; Zhang, M. *Biomaterials* **2002**, *23*, 1553.
(47) Duncan, R. *Nat. Rev. Drug Discovery* **2003**, *2*, 347.
(48) Farokhzad, O. C.; Langer, R. *ACS Nano* **2009**, *3*, 16.

■ NOTE ADDED AFTER ASAP PUBLICATION

This paper was published on January 12, 2016. The concentration noted in the experimental section for 2-methylimidazole has been corrected. The revised version was re-posted on January 27, 2016.

DOI: 10.1021/jacs.5b11720
J. Am. Chem. Soc. 2016, 138, 962−968